Bile acids contribute to the development of non-alcoholic steatohepatitis in mice

Justine Gillard, Laure-Alix Clerbaux, Maxime Nachit, Christine Sempoux, Bart Staels, Laure B. Bindels, Anne Tailleux, Isabelle A. Leclercq

Table of contents

Supplementary methods

BA analyses

To estimate total concentrations, BA were extracted from liver homogenates or 24h feces as described by Modica et al. [1] and quantified with Total Bile Acid Assay (Diazyme, DZ042A).

Oral glucose tolerance test

After 4 hours of fasting, mice were administered 40 mg of glucose by oral gavage. Blood glucose was measured at 0, 15, 30, 60, 90, 120 and 180 minutes after gavage using an Accu-Chek glucometer.

Fat mass and liver density

Whole body fat mass and liver density (normalized to spleen density) – a surrogate for liver steatosis [2] – were measured by micro computed tomography as previously described by Nachit et al. [3].

Histology and immunohistochemistry

Formalin-fixed, paraffin-embedded liver sections (4 µm thick) were stained with hematoxylin and eosin (H&E) or used for immunohistochemical detection of macrophages, neutrophils or cholangiocytes, using a polyclonal rat anti-mouse F4/80 antibody (1:200, AbD Serotec MCA497G) or Ly-6G (1:2000, BD Pharmingen 551459), or monoclonal rat anti-mouse CK19 (1/50, DSHB Troma III), a polyclonal rabbit anti-rat (1:100, Vector AI-4001) and Envision anti-rabbit-HRP (Dako K4003). The peroxidase activity was revealed with diaminobenzidine (Dako K3468) and sections counterstained with hematoxylin. Neutrophils were quantified as Ly6G+ area, and cholangiocytes as CK19+ area using Visiopharm software. NAFLD Activity score was assessed according to Kleiner et al. [4]. Liver sections were stained with picrosirius or sirius red to assess fibrosis.

RNA extraction, reverse transcription and real-time qPCR

RNA was extracted from snap frozen tissues using Trizol. cDNA was synthetized from 1 µg of RNA and gene expression assessed by quantitative polymerase chain reaction (Rotor-Gene Q, Qiagen). Ribosomal protein L19 (RPL19) was used as a reference gene to normalize the mRNA levels. Primer sequences are listed in Table S1.

Biochemical analyses

FGF15 protein concentrations were measured in portal plasma using a Mouse FGF15 ELISA kit (MyBioSource, MBS2019544). Insulin concentrations were measured in serum harvested

in 4h-fasted mice, using a Ultrasensitive Mouse Insulin ELISA kit (Mercodia, 10-1249-01). Plasma ALT and AST levels were measured using a DRI-CHEM NX500.

Anti-inflammatory test on RAW 264.7

RAW 264.7 macrophages (ATCC TIB-71) were cultured in DMEM containing 10% decomplemented FBS and 1% Penicillin/Streptomycin. At 80% of confluence in a 24 wells plate, medium was replaced by a FBS-free medium. One day later, cells were treated with FBS-free medium (CTL) or FBS-free medium containing TLCA 50 µM or 20% portal plasma for 2 hours. Cells were then exposed to LPS (1ng/ml) or vehicle. After three hours, cells were harvested in Trizol to extract RNA and TNFα gene expression was measured.

TGR5 functionality on BMDM

L929 cells (ATCC CCL-1) were cultured in DMEM containing 10% FBS, 1% HEPES and 1% Penicillin/Streptomycin for 10 days. The medium that contains M-CSF was harvested, filtered (100µm) and stored at -80°C.

Female WT and *foz/foz* mice (n=2/group) were killed and their femurs rapidly harvested in PBS at 4°C. Under a laminar flow, bone marrow was flushed out of the bones with PBS, filtered (70µm) and the filtrate was then centrifugated. The pellet was resuspended in RPMI containing 10% FBS, 1% Penicillin/Streptomycin and 10% L929 cells conditioned medium. Monocytes were diluted to obtain 2.5 million cells/mL and cultured for 8 days in the presence of L929-derived M-CSF to promote differentiation into macrophages.

After 8 days, the medium was replaced by a FBS-free medium and differentiated BMDM were exposed to vehicle or TLCA 100 µM. One hour later, BMDM were treated or not with LPS (1ng/mL). Two hours after LPS treatment, cells were harvested in Trizol to extract RNA and measure TNFα gene expression**.**

Hepatic bile flow

After a 12-hours overnight fasting, mice were anesthetized with ketamine-xylazine. The common bile duct was ligated, and the gallbladder cannulated with a catheter and then ligated. Bile was harvested for one hour, weighted and bile flow was expressed in volume per minute. Total BA concentration was then measured as described above to calculate BA quantity (µmol) per minute.

Supplementary figures

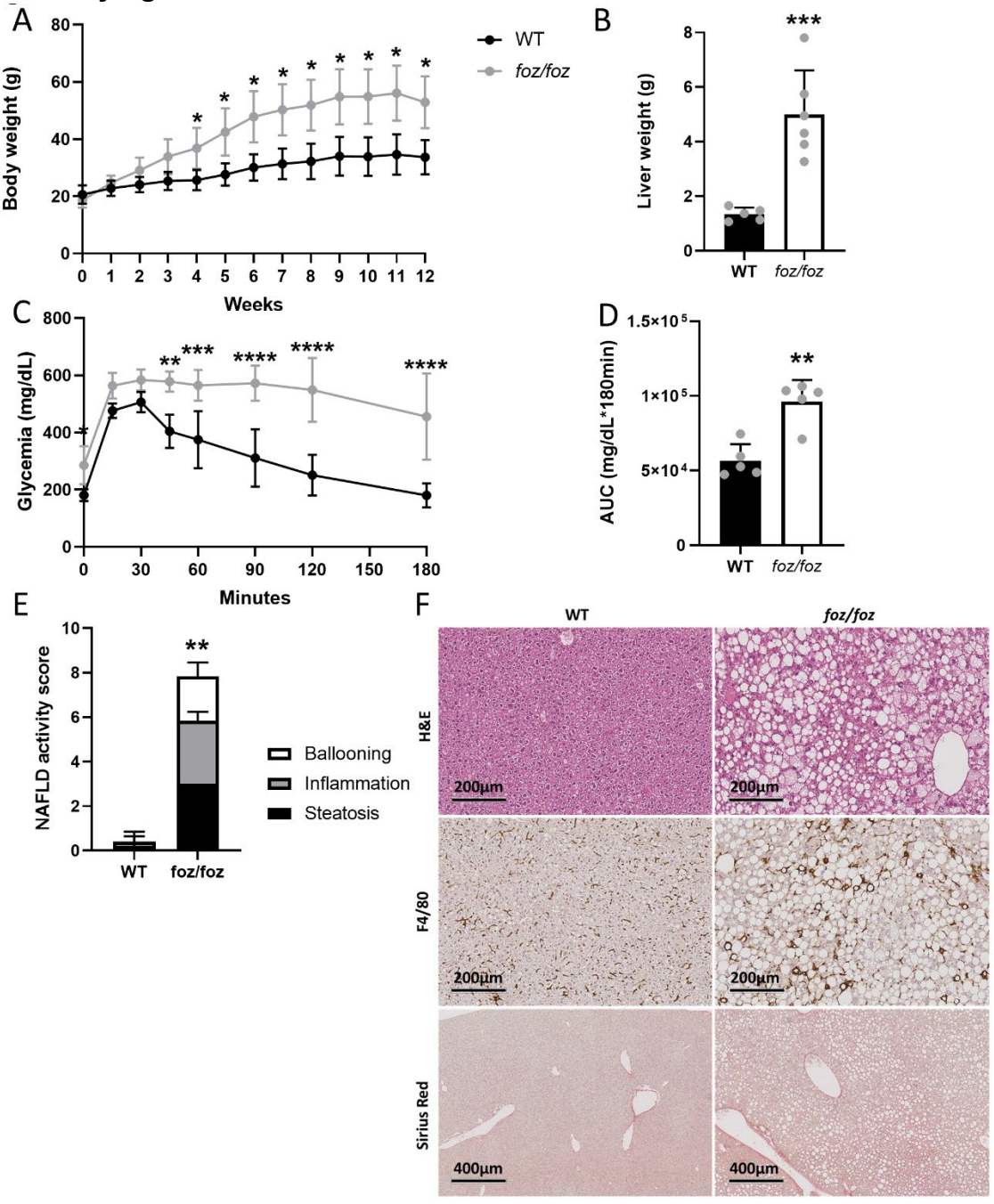

Fig. S1: HFD-fed *foz/foz* mice are a model of obesity, insulin resistance and NASH. (A) Body weight and (B) liver weight of *foz/foz* (n=6) and WT (n=5) mice fed a HFD for 12 weeks. (C) Glycemia during the OGTT performed at the end of the HFD feeding and (D) AUC of the glycemia over time. (E) NAFLD activity scores based on liver histology. (F) Representative H&E, F4/80 and sirius red staining of liver sections of WT and *foz/foz* mice fed a HFD for 12 weeks. Mean ± standard deviation. Unpaired two tailed t test for (B) and (D), Two-way ANOVA followed by post-hoc Bonferroni correction for (A) and (C) and Mann-Whitney test for (E): *p<0.05; **p<0.01, ***p<0.001 and **** p<0.0001.

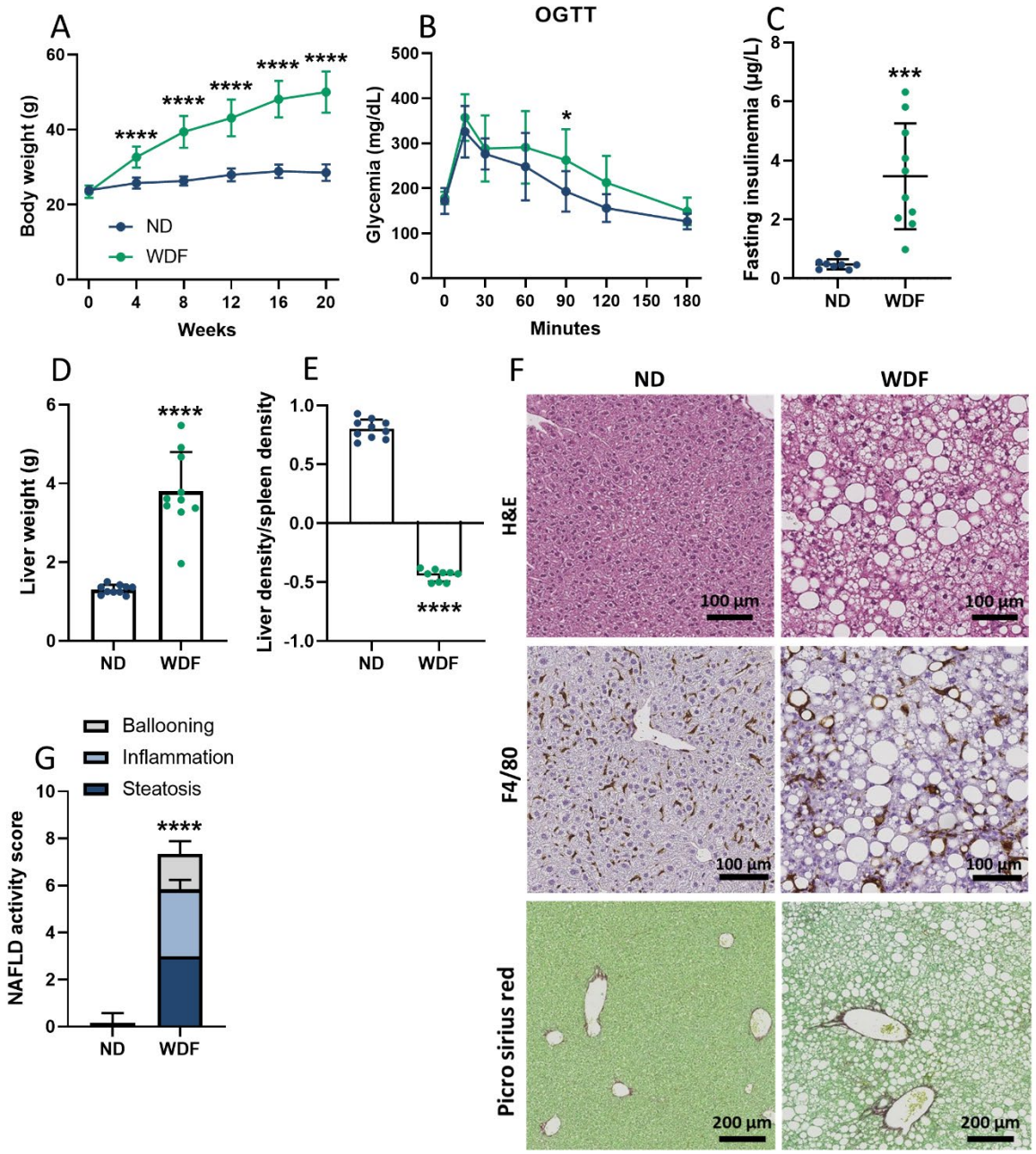

Fig. S2: Alterations in BA metabolism are not model specific. (A) Body weight, (B) glycemia during the OGTT, (C) fasting insulinemia, (D) liver weight and (E) density of C57BL/6J mice fed a ND or a WDF for 20 weeks (n=9-10/group). (F) Representative H&E, F4/80 and picrosirius red staining of liver sections and (G) histological NAFLD activity score. Mean ± standard deviation. Two-way ANOVA followed by post-hoc Bonferroni correction for (A) and (B), unpaired two tailed t test for (C), (D) and (E), Mann-Whitney test for (G): *p<0.05; ***p<0.001 and **** p<0.0001.

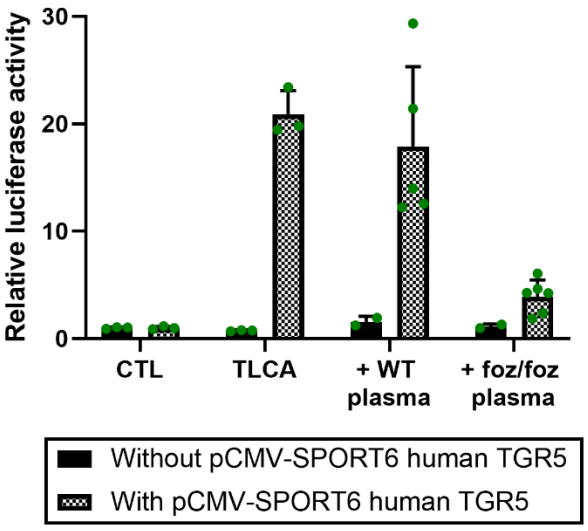

Fig. S3: Relative luciferase activity is TGR5-dependent. TGR5 activation by medium (CTL, n=3) or medium containing TLCA (used as a positive control, 10 µM, n=3), 20% portal plasma of WT (n=5) or *foz/foz* mice (n=6) in HEK293T cells. Results are expressed as firefly luminescence normalized to renilla luminescence. Mean ± standard deviation.

A

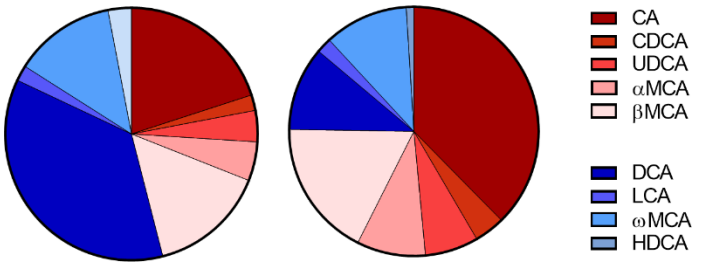

	WT	*foz/foz*	p-value
Primary BA	45.8±13.1%	75.2±8.7%	0.0032
Secondary BA	54.2±13.1%	24.8±8.7%	0.0032

B

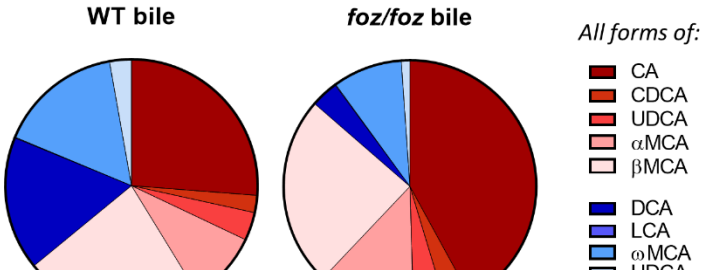

	WT	*foz/foz*	p-value
Primary BA	64.2±5.9%	86.5±4.1%	0.0001
Secondary BA	35.8±5.9%	13.5±4.1%	0.0001

C

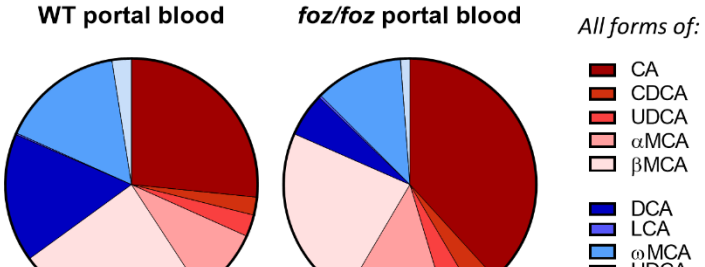

	WT	*foz/foz*	p-value
Primary BA	65.2±6.4%	81.7±6.5%	0.023
Secondary BA	34.8±6.4%	18.3±6.5%	0.023

Fig. S4: Relative BA composition is altered in (A) systemic blood, (B) bile and (C) portal blood of HFD-fed *foz/foz* and WT mice (n=4-6/group). CA, CDCA, UDCA, αMCA and βMCA are mouse primary BA and represented in red shades. DCA, LCA, ωMCA and HDCA are mouse secondary BA and represented in blue shades. Mean ± standard deviation. Unpaired two tailed t test.

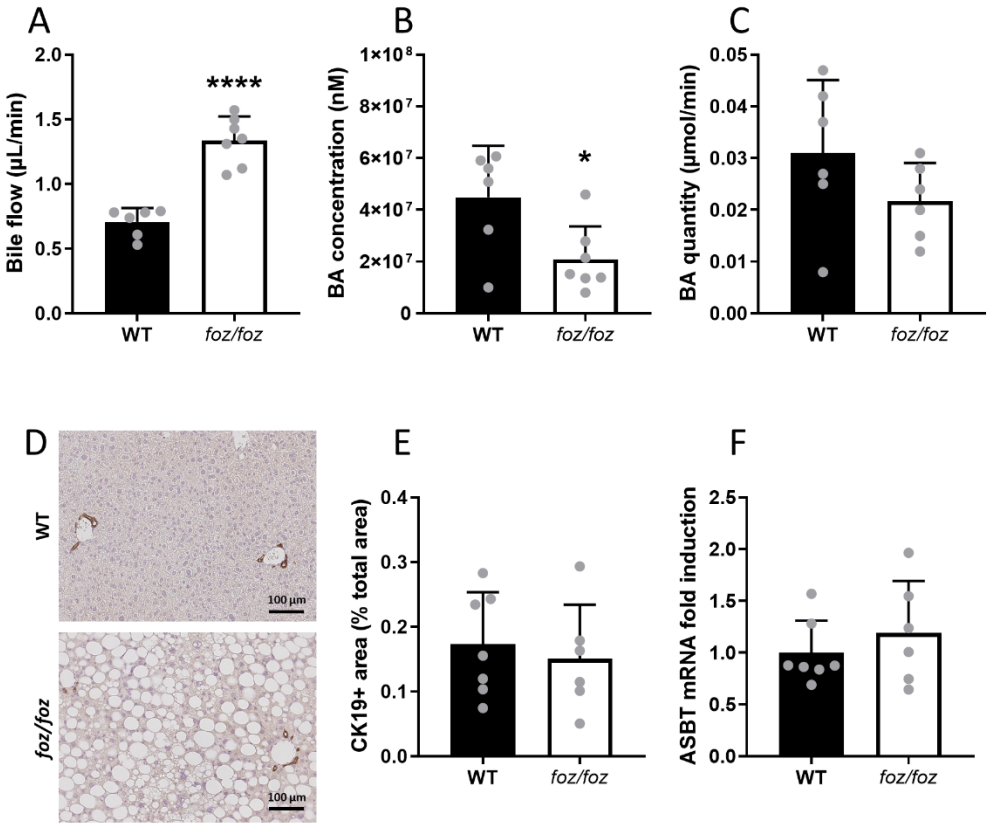

Fig. S5: *Alms1* mutation does not impact hepatic bile flow and cholangiocytes functionality in *foz/foz* mice. (A) Hepatic bile flow, (B) total BA concentration in bile harvested and (C) BA quantity secreted by the liver per unit of time in 12 weeks HFD-fed WT and foz/foz mice (n=6/group). (D) CK19 staining and (E) quantification, and (F) ASBT gene expression in the liver of 12 weeks HFD-fed WT and foz/foz mice (n=6-7/group). Mean ± standard deviation. Unpaired two tailed t test: *p<0.05 and **** p<0.0001.

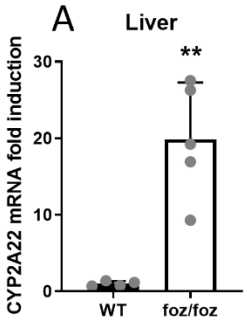

Fig. S6. (A) Hepatic CYP2A22 gene expression of HFD-fed *foz/foz* (n=4) and WT mice (n=5). Mean ± standard deviation. Unpaired two tailed t test: **p<0.01.

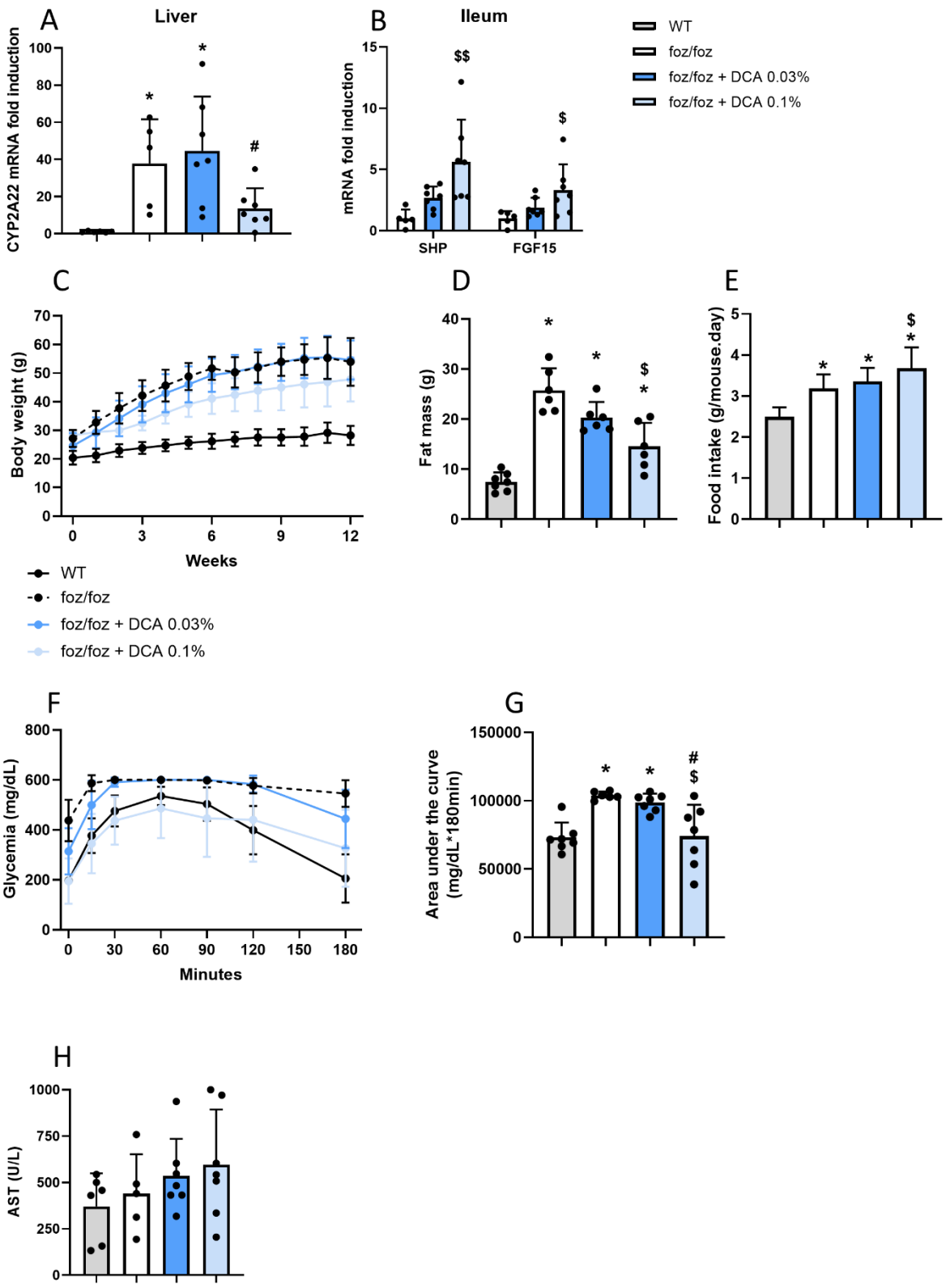

Fig. S7: Supplementation of the HFD with DCA 0.1% improves obesity and glucose tolerance in HFD-fed *foz/foz* mice. Gene expression of (A) of CYP2A22 in the liver and (B) of SHP and FGF15 in the ileum. (C) Body weight, (D) total fat mass and (E) mean food intake per mouse and per day of HFD-fed WT, *foz/foz*, *foz/foz* + DCA 0.03% and *foz/foz* + DCA

0.1% mice (n=5-7/group). (F) Glycemia during the OGTT performed at the end of the HFD feeding and (G) AUC of the glycemia over time (n=5-7/group). (H) Plasmatic alanine transaminase (AST) levels. Mean ± standard deviation. One-way ANOVA followed by post-hoc Bonferroni correction for (A), (B), (D), (E), (G) and (H). Statistical significance ($p<0.05$) is represented by * when compared to WT, $ when compared to *foz/foz* and # when compared to *foz/foz* + DCA 0.03%.

Supplementary table

Table S1. qPCR primer sequences.

Gene	Forward	Reverse
ASBT	TGGATAGATGGCGACATGGA	GGCAAGCAGTGTGGAGCAA
BSEP	CTGCCAAGGATGCTAATGCA	CGATGGCTACCCTTTGCTTCT
CYP27A1	GCCTCACCTATGGGATCTTCA	TCAAAGCCTGACGCAGATG
CYP2A12	AAGGCTATGGTGTGGATTC	GTAGATGGTGGGGTCAATGG
CYP2A22	GGGGACCGCTTCAACTACG	GTCCAGGGTACTGTGGTTGTG
CYP7A1	AGCAACTAAACAACCTGCCAGTACTA	GTCCGGATATTCAAGGATGCA
CYP7B1	TAGCCCTCTTTCCTCCACTCATA	GGCTGGCTTCCTGAGCTTATT
CYP8B1	GGCTGGCTTCCTGAGCTTATT	ACTTCCTGAACAGCTCATCGG
FABP6	GTGGAAAGTAGACCGGAACGA	GGAAGCAGCAGAAGCTTGGT
FGF15	GACCAAAACGAACGAAATTTGTT	ACGTCCTTGATGGCAATCG
FXR	AGGAGCCCCTGCTTGATGT	GCGGGTTCTCAGGCTGGTA
IL1β	AGTTGACGGACCCCAAAAGA	GGACAGCCCAGGTCAAAGG
MCP1	CCACTCACCTGCTGCTACTCAT	CTGCTGGTGATCCTCTTGT
NTCP	CTTGCGCCATAGGGATCTTC	TGCCTGCCTTGAGGACGTA
OSTα	CCGTCAAGCCAAGATGCAT	CAAGCACCTGGAACAGAGCAA
OSTβ	CCGGGGGAACCTGAGTAGAA	GTTATGGGGCGTTATGGGGT
RPL19	GAAGGTCAAAGGGAATGTGTTCA	CCTTGTCTGCCTTCAGCTTGT
SHP	AGGGTAGAGGCCATGAGGAG	ACGATCCTCTTCAACCCAGA
TGR5	GGCCTGGAACTCTGTTATCG	GTCCCTCTTGGCTCTTCCTC
TNFα	GTGCCTATGTCTCAGCCTCTT	GCTCATACCAGGGTTTGAGCT
VCAM1	AGTTGGGGATTCGGTTGTTCT	CCCCTCATTCCTTACCACCC

Supplementary references

[1] Modica S, Murzilli S, Moschetta A. Characterizing Bile Acid and Lipid Metabolism in the Liver and Gastrointestinal Tract of Mice. vol. 1. 2011. https://doi.org/10.1002/9780470942390.mo100226.

[2] De Rudder M, Bouzin C, Nachit M, Louvegny H, Vande Velde G, Julé Y, et al. Automated computerized image analysis for the user-independent evaluation of disease severity in preclinical models of NAFLD/NASH. Lab Investig 2020;100:147–60. https://doi.org/10.1038/s41374-019-0315-9.

[3] Nachit M, De Rudder M, Thissen JP, Schakman O, Bouzin C, Horsmans Y, et al. Myosteatosis rather than sarcopenia associates with non-alcoholic steatohepatitis in non-alcoholic fatty liver disease preclinical models. J Cachexia Sarcopenia Muscle 2020;32:1–15. https://doi.org/10.1002/jcsm.12646.

[4] Kleiner DE, Brunt EM, Van Natta M, Behling C, Contos MJ, Cummings OW, et al. Design and validation of a histological scoring system for nonalcoholic fatty liver disease. Hepatology 2005;41:1313–21. https://doi.org/10.1002/hep.20701.